Solar Cells, 8 (1983) 337 - 353

'roc. 3rd Pho-
be published.
ys. Lett., 40

61st Electro-

V. Palz (eds.),
voltaic Solar

IMPORTANCE OF THE EMITTER IN THIN BACK-SURFACE FIELD SOLAR CELLS

S. K. MEHTA and S. C. JAIN
Solid State Physics Laboratory, Lucknow Road, Delhi 110007 (India)

(Received May 5, 1982; accepted October 4, 1982)

Summary

The variation in the short-circuit current density J_{sc}, the open-circuit voltage V_{oc} and the efficiency η with the base thickness of an n^+–p–p^+ back-surface field (BSF) solar cell with a resistivity of 10 Ω cm is reported for 1 sun air mass 0 illumination. It was found that when the cell thickness is small the cell characteristics are determined by the properties of the emitter. The effects of different emitter dark saturation current densities J_{E0} and different base diffusion lengths L_B on the variation in V_{oc} with the change in base thickness were calculated. If the base diffusion length is taken to be equal to or greater than 1000 μm for $J_{E0} = 2 \times 10^{-12}$ A cm^{-2}, the calculated variation in V_{oc} with the base thickness is found to be in good agreement with the observed result that V_{oc} is independent of the cell thickness in the base thickness range 300 - 100 μm.

The calculations which were made for the case when a light reflector is present at the back of the BSF cell show that the maximum efficiency, which is obtained at a base thickness $w_B \approx 200$ μm, is appreciably increased.

The effective surface recombination velocity S_{eff} at the edge of the low–high junction is calculated as a function of the thickness w_H of the high region for various values of the recombination velocity S_r at the back contact. The calculations show that for $S_r > S_v$ (where S_v is the diffusion velocity in the high region and is equal to D_H/L_H, and D_H and L_H are the diffusion coefficient and the diffusion length of the high region respectively) small values of S_{eff} are obtained when the high region thickness w_H is greater than the high region diffusion length L_H ($w_H \approx 3L_H$). For $S_r = S_v$, S_{eff} is independent of the thickness of the high region and has a value given by $S_v N_B/N_H$; when $S_r < S_v$, the high region must be thin but the thickness must be larger than the depletion width of the low–high junction.

The temperature degradation coefficient of V_{oc} for a BSF cell was calculated with the band gap narrowing in both the emitter and the high region taken into account. The band gap narrowing in both these regions reduces the temperature degradation coefficient of V_{oc}.

0379-6787/83/0000-0000/$03.00

1. Introduction

A back-surface field (BSF) solar cell contains a highly doped region at the back of a low doped base, thereby forming a low–high (LH) junction. Gunn [1] has investigated the behaviour of the LH junction and has shown that it acts as a barrier to the flow of minority carriers from the low to the high side of the junction. At low injections this property of the LH junction is characterized by a leakage velocity which is equivalent to an effective surface recombination velocity S_{eff} at the edge of the LH junction. S_{eff} depends on the level of doping in the low and high regions and on the geometrical parameters of the high region. In cases of practical interest, S_{eff} is less than the surface recombination velocity at the back contact (see Section 5). This reduction in the recombination velocity S_{eff} at the back of the base leads to a reduction in the dark saturation current density J_0 and an increase in the short-circuit current density J_{sc} (see Section 2.1); consequently, the open-circuit voltage V_{oc} and the efficiency η increase.

Godlewski *et al.* [2] have used Gunn's theory of an LH junction to explain the experimental results of Mandelkorn and Lamneck [3] on BSF solar cells. They have calculated the base dark saturation current density J_{B0} using Gunn's theory [1] of an LH junction. In their calculations a value of 5×10^{-14} A cm^{-2} was used for the emitter dark saturation current density J_{E0} and a fixed value of 40 mA cm^{-2} was used for the short-circuit current density J_{sc} for all values of base thickness. Using a shifting approximation [4], they have calculated the open-circuit voltage V_{oc} for different values of the base thickness. These calculations have shown that an LH junction can indeed be used to give higher values of V_{oc} and higher efficiencies. The calculated variation in V_{oc} with the cell thickness did not, however, agree quantitatively with the experimental values. Since these calculations were made many papers have appeared on the BSF solar cell [5 - 8]. In a recent paper, Singh and Jain [5] have calculated the value of V_{oc} for different values of the base thickness. However, they have taken the emitter dark saturation current to be zero which increases the sensitivity of V_{oc} to the base thickness. Their calculated values of V_{oc} tend to infinity as the value of the base thickness becomes small. The results of the present paper show that the importance of the emitter dark saturation current in determining the V_{oc} of a BSF cell increases rapidly as the base thickness becomes small.* This is to be contrasted with the conventional cell in which V_{oc} tends to zero as w_{B} becomes vanishingly small, irrespective of the properties of the emitter.

In this paper, we present the results of our calculation of the variation in V_{oc} and η with the base thickness w_{B}, taking into account the variation in both J_{sc} and J_{B0} with w_{B} (a definition of these symbols is given in the

*Singh and Jain have used the low injection boundary condition when high injection conditions prevail. The correct high injection boundary condition has been given by Dhariwal *et al.* [9] and has been used by Sabnis [7] and by Grung [10].

Nomenclature). A constant value of 2×10^{-12} A cm^{-2} [11 - 13] for the emitter dark saturation current density J_{E0} was used for the above calculations (Section 2). In Section 3 the calculations made for a cell with a light reflector at the back are reported and in Section 4 we consider the effect of different values of J_{E0} and L_B on the variation in V_{oc} with base thickness.

The variation in S_{eff} with the thickness of the high region for various recombination velocities at the back contact is calculated in Section 5. In Section 6 the temperature degradation coefficient of V_{oc} is calculated with the band gap narrowing in both the emitter and the high region taken into account.

2. Effect of base thickness on the performance of a back-surface field solar cell

In this section we discuss the results of the calculation of the short-circuit current density J_{sc}, the open-circuit voltage V_{oc} and the efficiency η of a BSF solar cell for different values of base thickness. The values of the parameters used in these calculations are given in Table 1.

The short-circuit current density contribution from the emitter and the base was calculated using ref. 14, eqn. (4), and ref. 6, eqn. (6).

A value of 2×10^{-12} A cm^{-2} [11 - 13] was used for the emitter dark saturation current density. The expression for the base dark saturation current density J_{B0} and the open-circuit voltage V_{oc} is given below [2, 15]:

$$J_{B0} = \frac{qn_{io}^2 D_B}{N_B L_B} \left(\frac{S_{eff}}{D_B/L_B} + \tanh W_B \right) \left\{ 1 + \left(\frac{S_{eff}}{D_B/L_B} \right) \tanh W_B \right\}^{-1} \quad (1a)$$

for $S_{eff} = 0$

$$J_{B0} = \frac{qn_{io}^2 D_B}{N_B L_B} \tanh W_B \quad (1b)$$

TABLE 1

Values of the parameters used in the calculations in Section 2

Base resistivity (p type)	10 Ω cm
Base width	Variable
Diffusion length L_B in the base	1000 μm
Effective surface recombination velocity S_{eff} at the edge of the LH junction	0
Emitter saturation current density (at 300 K)	2×10^{-12} A cm^{-2} [a]
Average doping in the emitter (n type)	10^{20} cm^{-3}
Front-surface recombination velocity S_F	5×10^4 cm s^{-1}
Junction depth	0.5 μm

[a] See refs. 11 - 13.

$$V_{oc} \approx \frac{kT}{q} \ln\left(\frac{J_{scB} + J_{scE}}{J_{B0} + J_{E0}}\right) \approx \frac{kT}{q} \ln\left(\frac{J_{sc}}{J_0}\right) \tag{2}$$

The expressions for V_{mp} and J_{mp} are given by [15]:

$$\left(1 + \frac{qV_{mp}}{kT}\right) \exp\left(\frac{qV_{mp}}{kT}\right) = \frac{J_{sc}}{J_0} + 1 \tag{3a}$$

$$J_{mp} = \frac{V_{mp} J_0}{kT/q} \exp\left(\frac{qV_{mp}}{kT}\right) \tag{3b}$$

The power output for 1 sun air mass (AM) 0 illumination (135.3 mW cm^{-2}) is obtained from the product of V_{mp} and J_{mp}. The efficiency η can easily be calculated.

2.1. The case of monochromatic light

The variation in J_{sc} and V_{oc} with the base thickness is shown in Fig. 1 for monochromatic light. Curves 1 and 2 show the variation in J_{sc} with w_B for different values of the absorption coefficient: $\alpha = 100$ cm^{-1} for curve 1 and $\alpha = 1000$ cm^{-1} for curve 2. For $w_B \gtrsim 2500$ μm the values of J_{sc} are the same as those for an infinitely thick cell and are independent of the nature

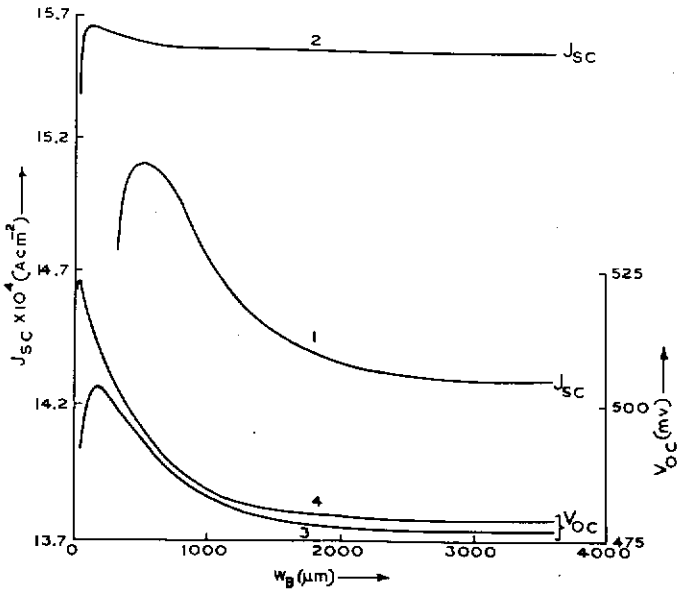

Fig. 1. J_{sc} (curves 1 and 2) and V_{oc} (curves 3 and 4) plotted as a function of the base thickness w_B for monochromatic light (absorption coefficient: curve 1, $\alpha = 100$ cm^{-1}; curve 2, $\alpha = 1000$ cm^{-1}; curve 3, $\alpha = 100$ cm^{-1}; curve 4, $\alpha = 1000$ cm^{-1}).

of the back
maximum at
seen from F
maximum is
smaller wavel

The var
maximum fo
physical cons
normalized c
a semi-infinit
current with
monochroma
at $w_B \approx 500$
at different
junction is pl

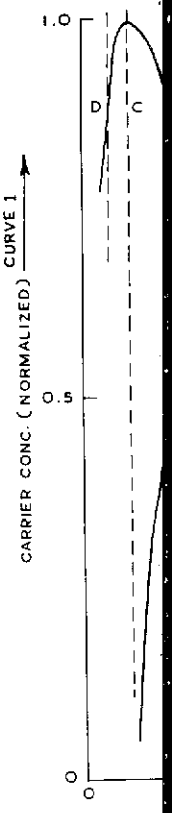

Fig. 2. Curve 1
with a thick b
circuit current

of the back contact. As w_B is reduced, J_{sc} first increases and then becomes a maximum at a particular value of w_B before starting to decrease. It can be seen from Fig. 1, curves 1 and 2, that the value of w_B at which J_{sc} is a maximum is smaller for larger absorption coefficients or for incident light of smaller wavelength.

The variation in J_{sc} with w_B, and in particular the fact that J_{sc} has a maximum for a particular value of w_B, can be understood from general physical considerations with the aid of Fig. 2. Figure 2, curve 1, shows the normalized carrier profile in the short-circuit configuration for a diode with a semi-infinite base [16]. Curve 2 shows the variation in the short-circuit current with the base thickness of a BSF solar cell. The incident light is monochromatic and $\alpha = 100\ \text{cm}^{-1}$. The short-circuit current has a maximum at $w_B \approx 500\ \mu\text{m}$. Let us now consider the effect of putting the LH junction at different positions on the carrier profile given by curve 1. When the LH junction is placed at position A, the slope in the carrier profile at position A

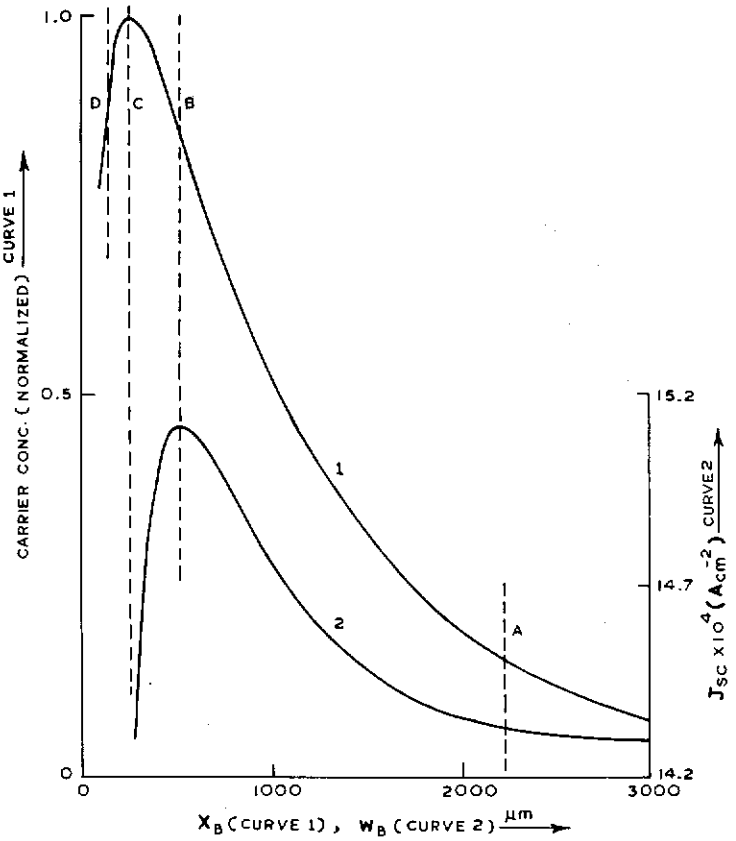

Fig. 2. Curve 1, the normalized carrier profile under short-circuit conditions in a solar cell with a thick base ($\alpha = 100\ \text{cm}^{-1}$ (*i.e.* $\lambda \approx 1.0\ \mu\text{m}$)); curve 2, the variation in the short-circuit current with base thickness w_B ($\alpha = 100\ \text{cm}^{-1}$).

will change from a finite negative value to zero (as $S_{eff} = 0$). The carriers which were previously flowing towards the back ohmic contact will now be reflected towards the junction. A large fraction of these carriers will recombine on the way to the junction but a small number will reach the junction, increasing J_{sc}. It can be seen from Fig. 2 that the slope of the profile (curve 1) increases from position A towards the junction. As the LH junction is moved from position A towards the junction, the number of reflected carriers increases. Also, the fraction of the reflected carriers which reach the junction increases because the carriers now have to travel a shorter distance and so the fraction lost by recombination becomes smaller. As a result, J_{sc} increases continuously with the decrease in base thickness from position A to position B. Between positions B and C the slope of the carrier profile decreases rapidly. As the LH junction is moved from B to C, the number of reflected carriers also decreases and J_{sc} starts to decrease. It should be noted, however, that the short-circuit current for base thicknesses between B and C is still greater than that for an infinitely thick cell. When the LH junction is at position C, the carrier profile between C and the junction remains unaffected by the LH junction because the slope of the profile was zero at C before the LH junction was placed there and the LH junction does not change the carrier profile. Therefore, at this cell thickness the J_{sc} obtained with a BSF cell is equivalent to that for an infinitely thick cell. Finally, as the position of the LH junction is moved closer to the junction (say to position D), the short-circuit current decreases rapidly and becomes smaller than that for an infinitely thick cell. This happens because the carriers generated between D and C which previously reached the junction are lost when the distance becomes equal to the thickness at position D. It should be noted that the effects of carriers generated in the high region have been neglected in the present work as well as in previous models [2, 17].

We shall now discuss the values of V_{oc} for the BSF cell as shown in Fig. 1, curves 3 and 4. V_{oc} shows the same qualitative behaviour as J_{sc}. It should be noted, however, that the maxima of V_{oc} and J_{sc} occur at different values of w_B for the same value of α. The reason for this difference in the position of the maxima is not difficult to understand and can be seen from eqn. (2). The value of the short-circuit current from the base is not influenced by the properties of the emitter. It is easy to see that, if S_{eff} is equal to zero, both J_{scB} and J_{B0} tend to zero for very small values of w_B. Equation (2) shows that for a very thin BSF cell V_{oc} is determined by the short-circuit current density J_{scE} and the dark saturation current density J_{E0} in the emitter; the limiting value of V_{oc} is given by

$$V_{oc} \approx \frac{kT}{q} \ln\left(\frac{J_{scE}}{J_{E0}}\right) \tag{4}$$

The diode is now emitter dominated. The actual position of the maximum in the V_{oc} curve depends on the numerical values of J_{B0} and J_{E0} used in eqn. (2).

In a conventional cell, J_{B0} becomes infinity as w_B and V_{oc} tend to zero. The emitter plays no role in a very thin conventional cell, whereas it plays a

dominant rol
w_B is small b
J_{E0}. V_{oc} will n

$$V_{oc} \approx \frac{kT}{q} \ln$$

and will have

2.2. The case

When w
density due
circuit curre
1 sun AM 0
lengths is car

In Fig.
base thickne
J_{sc} has been
However, the
This can eas
values of α, a

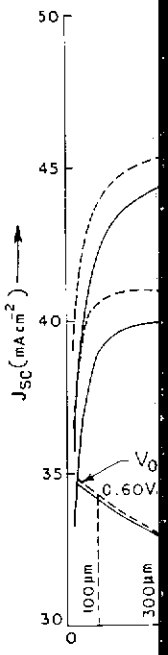

Fig. 3. J_{sc} (cur
w_B (illuminati
taking BSR int

dominant role in a thin BSF cell. If for a conventional cell the base thickness w_B is small but finite, then J_{SCE} is greater than J_{SCB} and J_{B0} is greater than J_{E0}. V_{oc} will now be given for a conventional cell by

$$V_{oc} \approx \frac{kT}{q} \ln\left(\frac{J_{SCE}}{J_{B0}}\right) \tag{5}$$

and will have a very small value.

2.2. The case of 1 sun air mass 0 illumination

When white light is incident on a solar cell, the short-circuit current density due to different wavelengths combines to yield the total short-circuit current density. To calculate the short-circuit current density for 1 sun AM 0 illumination, the summation of J_{sc} for the constituent wavelengths is carried out using the method of Wolf [18].

In Fig. 3, curve 1 (full curve), the calculated variation in J_{sc} with the base thickness is shown for 1 sun AM 0 light. It can be seen that although J_{sc} has been integrated it still has a maximum at a base width of 600 μm. However, the maximum is now broad and is less prominent than before. This can easily be understood from the J_{sc} *versus* w_B plot for different values of α, as shown in Fig. 1. The maximum values of J_{sc} are at different

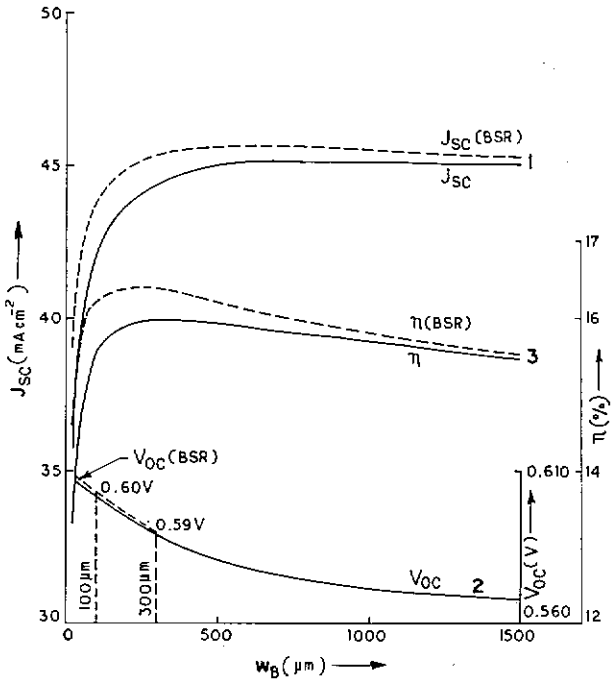

Fig. 3. J_{sc} (curves 1), V_{oc} (curves 2) and η (curves 3) as a function of the base thickness w_B (illumination, 1 sun AM 0): ——, ignoring back-surface reflection (BSR); — — —, taking BSR into account.

values of w_B for different wavelengths and therefore the maximum is broadened in the summation over all the wavelengths of the spectrum. The position and sharpness of the maximum depends on the spectral composition of the incident light.

The calculated variation in V_{oc} with w_B is shown in Fig. 3, curve 2 (full curve). It can be seen that V_{oc} increases continuously as the base thickness w_B decreases; however, the increase in voltage with decreasing thickness is much smaller than that calculated by Godlewski *et al.* [2]. Our analysis shows that for base thicknesses between 300 and 100 μm (the range of practical interest) the increase in V_{oc} is only 0.01 V. This explains the observed result [3] that the V_{oc} of a BSF cell with a resistivity of 10 Ω cm is independent of the base thickness in the range 300 - 100 μm. If the base thickness is decreased to less than 10 μm, V_{oc} starts to decrease and ultimately attains a value determined by the ratio of the emitter short-circuit current to the emitter dark saturation current. (This is not shown in Fig. 3.) However, the contribution of the high region, which is usually ignored [2, 17], may in this case become appreciable.

The calculated variation in the efficiency is shown in Fig. 3, curve 3 (full curve). It can be seen that the efficiency has a maximum at $w_B \approx 200$ μm. The change in the efficiency for base thicknesses in the range 300 - 100 μm is 0.4%; the efficiency therefore remains constant within the experimental error for this range of base thickness.

3. The case of 1 sun air mass 0 illumination with a light reflector at the back of the cell

We have calculated the performance of a BSF cell with a mirror at the same place as the LH junction by using the method of Jain and Jain [19] for thin conventional solar cells. These authors have neglected to account for the absorption of light in the emitter. When the absorption of light in the emitter is taken into account, the base short-circuit current density can be written as

$$J_{SCB}(\text{refl}) = \frac{qFC_B}{1 - C_B^2} \exp\{-\alpha(2w_B + w_E)\} \times \times \{C_B + \tanh W_B - C_B \exp(C_B W_B) \operatorname{sech} W_B\} \quad (6)$$

We shall now calculate the increase in the emitter short-circuit current density J_{SCE} due to the back-reflected light. The boundary conditions used to solve the diffusion equation for this part of J_{SCE} are

$$P_E(0) = 0 \quad (7)$$

at all times. The distances are measured from the n^+–p junction and are positive in the base and negative in the emitter. At the front surface of the emitter at $x = -w_E$

$$D_E \frac{dP_E(x)}{dx}\bigg|_{x=-w_E} = S_F P_E(-w_E) \tag{8}$$

at all times. The generation rate for the reflected light is given by

$$G_{r\lambda}(\text{refl}) = \alpha(\lambda)F(\lambda)\exp\{-\alpha(w_E + 2w_B - x)\} \tag{9}$$

The expression for $J_{SCE}(\text{refl})$ which is determined by solving the diffusion equation using the boundary conditions given by eqns. (7) and (8) is as follows:

$$J_{SCE}(\text{refl}) = \frac{qFC_E \exp\{-\alpha(2w_B + w_E)\}}{1 - C_E^2} \times \left\{-C_E + \frac{(1+S_F')\exp(W_E) - (1-S_F')\exp(-W_E) - 2(S_F' - C_E)\exp(-C_E W_E)}{(1+S_F')\exp(W_E) + (1-S_F')\exp(-W_E)}\right\} \tag{10}$$

It should be noted that the mirror is considered to be in the same position as the LH junction. However, in a practical solar cell the reflector is placed at the back contact and not at the LH junction. As long as the thickness of the high region is negligibly small in comparison with the thickness of the base region, the error incurred by making this assumption is small.

For the sake of simplicity, we took the reflection coefficient to be unity in AM 0 light, for all wavelengths. The values of the parameters used in the calculations are the same as those given in Table 1.

The total amount of improvement in the short-circuit current density due to the presence of a light reflector at the back contact is the sum of $J_{SCB}(\text{refl})$ and $J_{SCE}(\text{refl})$, which are given by eqns. (6) and (10) respectively. It can be shown from numerical calculations that the value of $J_{SCE}(\text{refl})$ is negligible unless the base thickness is very small and the wavelength is large.

The calculated variations in J_{sc}, V_{oc} and the efficiency η with the base thickness are shown in Fig. 3 (broken curves). It can be seen from Fig. 3, curve 1 (broken curve), that the magnitude of the improvement in J_{sc} is greater for small base thicknesses than it is for larger base thicknesses. At $w_B \approx 100$ μm the improvement in J_{SC} is 4.5%, whereas for $w_B > 1500$ μm J_{sc} remains practically the same as it was without a back reflector. At larger base thicknesses a larger fraction of the light is absorbed before reflection and hence only a small portion is reflected back and can contribute to the improvement in the short-circuit current density.

Figure 3, curve 2 (broken curve), shows that V_{oc} increases slightly for $w_B < 200$ μm due to back-reflected light.

It can be seen from Fig. 3, curve 3 (broken curve), that the presence of a light reflector at the back of the cell gives an appreciable improvement in the cell efficiency η at the base thickness which corresponds to the maximum efficiency ($w_B \approx 200$ μm); the efficiency improves from 16.0% to 16.4%.

At smaller base thicknesses the improvement in efficiency is much larger than 0.4%. Qualitatively, these results are also in agreement with other experiments [20] that have been reported for BSF solar cells with a light reflector at the back contact. A BSF cell with an LH junction alone has the disadvantage that an appreciable portion of the incident light is not absorbed in the base because the base is so thin. With a light reflector the light which reaches the back contact is reflected back and this increases the effective thickness available for the absorption of light by a factor of 2. However, the actual gain in J_{sc} is greater than the value that would be obtained by increasing the thickness by a factor of 2 [19].

4. Effect of varying the cell parameters on the characteristics of a back-surface field solar cell

From the above calculations it can be seen that the open-circuit voltage and the power output of a BSF solar cell agree with the results determined experimentally [3] for $L_B = 1000$ μm, $J_{E0} = 2 \times 10^{-12}$ A cm^{-2} and $S_{eff} \approx 0$. More detailed calculations show that, if S_{eff} is not zero but has a small finite value (less than about 50 cm s^{-1}), the characteristics of the cell do not change appreciably. However, if S_{eff} is considerably larger, say 1000 cm s^{-1} or more, the theoretically calculated output characteristics become inferior. The simple calculations using Gunn's theory [1] show that the value of S_{eff} for the levels of doping used in the base and the high region is not likely to be large (see Section 5). The diffusion length in the base and the emitter dark saturation current are more important parameters. The calculated values of V_{oc} for base widths of 100 and 300 μm are shown in Table 2 for two different values of L_B and four different values of J_{E0}. It can be seen from Table 2 that, for a value of J_{E0} of 10^{-11} A cm^{-2} or more, the value of

TABLE 2

Calculated values of V_{oc} for base widths of 100 and 300 μm at various values of L_B and J_{E0}

L_B (μm)	J_{E0} (A cm^{-2})	V_{oc} (mV) *at the following values of* w_B	
		100 μm	*300 μm*
230	10^{-12}	581.1	559.3
	10^{-11}	557.4	547.5
	10^{-10}	507.2	507.8
	2×10^{-12}	577.1	557.0
1000	10^{-12}	611.4	594.6
	10^{-11}	568.9	565.7
	10^{-10}	512.0	512.9
	2×10^{-12}	601.5	589.3

V_{oc} for base thicknesses in the range 300 - 100 μm is smaller than the observed value of V_{oc} (600 mV) when L_B is between 230 and 1000 μm. Therefore these combinations of values of J_{E0} and L_B are not acceptable. For $J_{E0} = 2 \times 10^{-12}$ A cm^{-2} (the value which was used in the calculations of the plots in Fig. 3) the difference in V_{oc} for base thicknesses in the range 300 - 100 μm for $L_B = 1000$ μm is 12 mV; this is in contrast with a difference of 20 mV found previously for $L_B = 230$ μm. The calculated results are in better agreement with those determined experimentally [3] for larger values of L_B but the discrepancy for smaller values of L_B also appears to be within the range of experimental error.

From the experiments of Weaver and Nasby [21] it has been suggested that the bulk diffusion length in a BSF cell is much larger than that in a conventional cell. Recent experiments to determine the diffusion lengths in a BSF and a conventional cell fabricated in our laboratory showed similar results. It appears that the process of forming an LH junction on the back contact of a cell does improve the bulk diffusion length, in addition to reducing the effective value of the surface recombination velocity. The mechanism of improvement is probably the gettering action [21]. The improvement in the characteristics of the BSF cell is therefore due to both the reduction in the value of S_{eff} and the improvement in the value of L_B.

5. Effective surface recombination velocity at the edge of the low–high junction as a function of the thickness of the high region

The thickness of the high region has a large effect on the value of S_{eff}. Del Alamo *et al.* [22] have suggested that, in order to make S_{eff} small, the thickness of the high region should be made much larger than the diffusion length L_H; in contrast, Michel *et al.* [23] have suggested that the thickness of the high region should be smaller than L_H. In order to resolve this controversy we calculated the effect of the thickness w_H of the high region on S_{eff} for various values of the parameters of the high region. According to Gunn's theory [1], S_{eff} is given by

$$S_{eff} = \frac{N_B S_v}{N_H} \left\{ \frac{S_r/S_v + \tanh(w_H/L_H)}{1 + (S_r/S_v)\tanh(w_H/L_H)} \right\} \tag{11}$$

Taking $N_B/N_H = 10^{-4}$, $S_v = D_H/L_H = 1600$ cm s^{-1} and using eqn. (11), we calculated values of S_{eff} as a function of the reduced thickness W_H of the high region for various values of the recombination velocity S_r at the back contact. The results are shown in Fig. 4. There are three cases of practical importance, namely $S_r > S_v$, $S_r = S_v$ and $S_r < S_v$. It is convenient to discuss the dependence of S_{eff} on the thickness of the high region separately for the three cases.

5.1. $S_r > S_v$

It can be seen from Fig. 4, curves 1 and 2, that S_{eff} decreases as W_H increases. At small values of W_H, S_{eff} is large and approaches the value

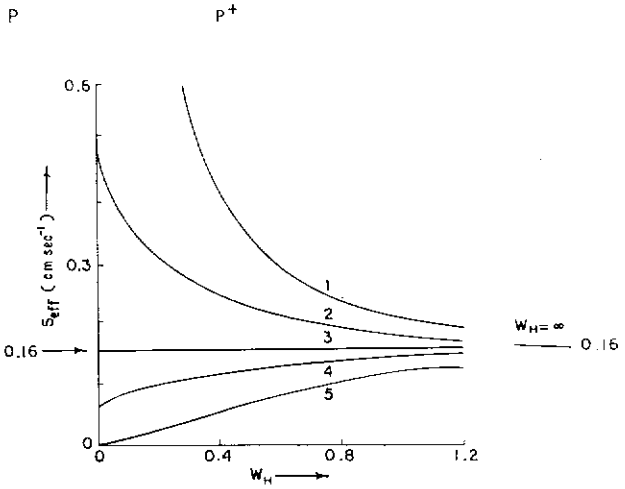

Fig. 4. S_{eff} is plotted as a function of the reduced thickness W_H of the high region for various values of the normalized surface recombination velocity S at the back ($S = S_r/S_v$): curve 1, $S = \infty$; curve 2, $S = 3$; curve 3, $S = 1$; curve 4, $S = 0.5$; curve 5, $S = 0$.

$S_r N_B/N_H$ as the thickness of the high region is decreased to zero. For large values of W_H ($W_H \gtrsim 3$), S_{eff} approaches a limiting value of $S_v N_B/N_H$. It should be noted that when $W_H \approx 3$ or more S_r has no effect on S_{eff}; the value of S_{eff} is determined entirely by recombinations in the bulk of the high region and S_{eff} is proportional to S_v.

5.2. $S_r = S_v$

In Fig. 4, curve 3, it is shown that, when $S_r = S_v$, S_{eff} is independent of the thickness of the high region. If $S_r = S_v$ is put into eqn. (11), the value of S_{eff} is found to be $S_v N_B/N_H$; this is identical with the value obtained in Section 5.1 for large values of W_H.

5.3. $S_r < S_v$

For $S_r < S_v$ the value of S_{eff} increases as W_H increases, as shown in Fig. 4, curves 4 and 5. If $W_H \gtrsim 3$, S_{eff} again becomes $S_v N_B/N_H$. To obtain a better performance and to reduce the value of S_{eff}, W_H must be made small. This result is the opposite of that obtained in Section 5.1 above. If we put $W_H = 0$ into eqn. (11), we find that the limiting value of S_{eff} for this case is $S_r N_B/N_H$.

We can see that the minimum limiting value of S_{eff} in Sections 5.1 and 5.2 is given by $S_v N_B/N_H$ and that it is given by $S_r N_B/N_H$ in Section 5.3. These values correspond to $W_H \gtrsim 3$ in Section 5.1, to all values of W_H in Section 5.2 and to W_H approaching zero in Section 5.3. Before concluding this section, we must point out that W_H is measured from the edge of the depletion layer. If the thickness of the high region is smaller than the mean free path of the electrons, then eqn. (11), which is derived by assuming a

diffusion-based transport across the junction, does not hold. It follows that we cannot obtain a reduction in the value of S_{eff} by making the high region thinner than the mean free path. This therefore puts a lower limit on the size of the thickness of the high region that can be used to obtain the minimum value of S_{eff} in Section 5.3, *i.e.* when $S_r < S_v$.

For small values of W_H, eqn. (11) can be written in the form

$$S_{eff} = \frac{N_B S_r}{N_H}\left\{1 + \frac{w_H}{L_H}\left(\frac{S_v}{S_r} - \frac{S_r}{S_v}\right)\right\} \tag{12}$$

In practice, the limiting value of S_{eff} can be calculated by putting w_H equal to the mean free path in the above equation.

6. Temperature degradation of V_{oc}

Mandelkorn and Lamneck [24] have observed that the temperature degradation of the open-circuit voltage of a BSF solar cell is less than that of a conventional solar cell. Sinha and Chattopadhyaya [25] have calculated the temperature degradation coefficient of the open-circuit voltage (which equals dV_{oc}/dT) of a BSF and a conventional cell theoretically. However, they have not considered the effect of the emitter band gap narrowing in their calculations. In this paper, we calculated the degradation coefficient of V_{oc}, taking into account the band gap narrowing in the emitter and in the high region at the back of the cell. For simplicity, we assumed that the doping in the emitter, as well as in the high region, is uniform. We also assumed that the effect of a change in the short-circuit current with temperature on the temperature variation in V_{oc} is negligible (see ref. 26 for a discussion of this assumption).

The open-circuit voltage was calculated using eqn. (2) and eqns. (A3), (A4) and (A5) for different cell temperatures. These equations are the same as those given in refs. 15 and 16; they are rewritten in Appendix A in order to show the explicit temperature dependence. We took $w_B = 150$ μm and $J_{sc} = 45$ mA cm^{-2}; the other parameters used are the same as those given in Table 1. The calculated variation in V_{oc} with temperature is shown in Fig. 5. In Fig. 5, curve 1, the band gap narrowing is neglected in both the emitter and the high region. For curve 2, we took a value of 0.11 eV (which corresponds to a level of doping of about 10^{19} cm^{-3}) [11] for the band gap narrowing in the high region and a value of 0.16 eV (which corresponds to a level of doping of about 10^{20} cm^{-3}) [11] for the band gap narrowing in the emitter. The effective surface recombination velocity at 300 K for both curves was taken to be equal to the realistic value of 50 cm s^{-1}. From Fig. 5 it is clear that the band gap narrowing in the emitter and the high region reduces the temperature dependence of V_{oc}. The value of the degradation coefficient of V_{oc} is indicated on the curves. We also calculated the degradation coefficient for the following cases: (a) the band gap narrowing in the high region was neglected and that in the emitter was taken to be equal to

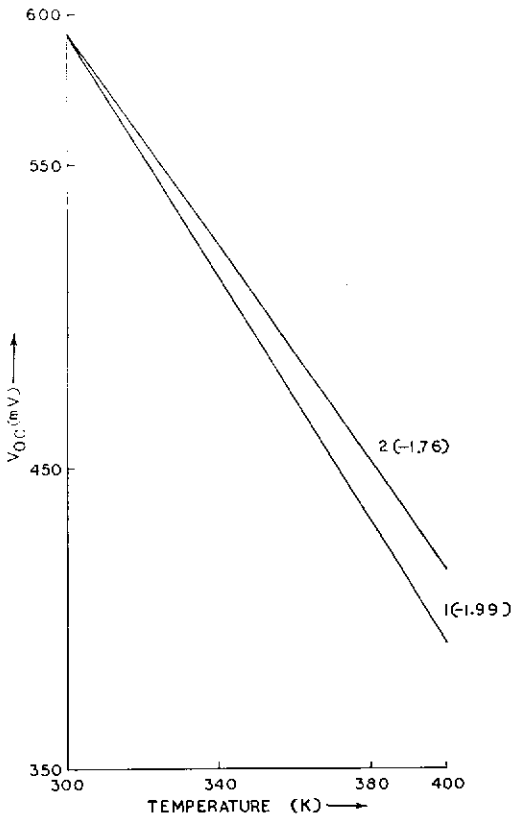

Fig. 5. V_{oc} as a function of the temperature of a BSF cell with the band gap narrowing neglected in both the emitter and the high region (curve 1) and with the band gap narrowing taken to be 0.16 eV in the emitter and 0.11 eV in the high region (curve 2): S_{eff} = 50 cm s^{-1} at 300 K; the value of the degradation coefficient of V_{oc} is indicated on the curves.

0.16 eV; (b) the band gap narrowing in the emitter was neglected and that in the high region was taken to be equal to 0.11 eV. The values of the degradation coefficient of V_{oc} for cases (a) and (b) are -1.87 mV K^{-1} and -1.92 mV K^{-1} respectively.

Nomenclature

C	αL, product of the absorption coefficient and the diffusion length
D	diffusion coefficient
E_g	energy band gap of silicon
F	incident light flux
J_{mp}	current density at maximum power point
J_{sc}	short-circuit current density
J_0	dark saturation current density
k	Boltzma
L	diffusio
n_{ie}	intrinsic
n_{io}	intrinsic
N	doping
p	excess h
q	electron
S_{eff}	effectiv
	gap nar
S_{eff}'	effectiv
	narrowi
S_F,	front-su
S_F	$S_F/(D_E$
S_r	back-su
S_v	D_H/L_H
T	tempera
V_{mp}	open-ci
V_{oc}	open-ci
w	width
W	w/L, re
α	absorpt
ΔE_g	energy
η	convers

Subscripts

B	base
E	emitter
H	high re
λ	monoc

References

1 J. B. Gunn
2 M. P. Go
Specialists
p. 40.
3 J. Mandell
Alto, CA,
4 F. A. Lin
(1979) 16
5 S. N. Sing
6 A. Sinha
7 A. G. Sab
8 C.-Y. Wu
9 S. R. Dha
504.
10 B. L. Gr
IEEE, Ne
11 H. P. D. L

k	Boltzmann constant
L	diffusion length
n_{ie}	intrinsic carrier concentration with band gap narrowing
n_{io}	intrinsic carrier concentration without band gap narrowing
N	doping concentration
p	excess hole concentration
q	electronic charge
S_{eff}	effective surface recombination velocity at the edge of LH junction without band gap narrowing in the high region
S_{eff}'	effective surface recombination velocity at the edge of LH junction with band gap narrowing in the high region
S_F	front-surface recombination velocity
S_F'	$S_F/(D_E/L_E)$, normalized front-surface recombination velocity
S_r	back-surface recombination velocity
S_v	D_H/L_H, diffusion velocity of high region
T	temperature (K)
V_{mp}	open-circuit voltage at the maximum power point
V_{oc}	open-circuit voltage
w	width
W	w/L, reduced width
α	absorption coefficient
ΔE_g	energy band gap narrowing
η	conversion efficiency

Subscripts

B	base
E	emitter
H	high region
λ	monochromatic light

gap narrowing
id gap narrow-
urve 2): S_{eff} =
dicated on the

ted and that
alues of the
mV K^{-1} and

References

1 J. B. Gunn, *J. Electron. Control, 4* (1958) 17.
2 M. P. Godlewski, C. R. Baraona and H. W. Brandhorst, Jr., *Proc. 10th Photovoltaic Specialists' Conf., Palo Alto, CA, November 13 - 15, 1973*, IEEE, New York, 1974, p. 40.
3 J. Mandelkorn and J. H. Lamneck, Jr., *Proc. 10th Photovoltaic Specialists' Conf., Palo Alto, CA, November 13 - 15, 1973*, IEEE, New York, 1974, p. 207.
4 F. A. Lindholm, J. G. Fossum and E. L. Burgess, *IEEE Trans. Electron Devices, 26* (1979) 165.
5 S. N. Singh and G. C. Jain, *Sol. Cells, 5* (1982) 143.
6 A. Sinha and S. K. Chattopadhyaya, *Solid-State Electron., 21* (1978) 943.
7 A. G. Sabnis, *Solid-State Electron., 21* (1978) 581.
8 C.-Y. Wu and W.-Z. Shen, *Solid-State Electron., 23* (1980) 209.
9 S. R. Dhariwal, L. S. Kothari and S. C. Jain, *IEEE Trans. Electron Devices, 23* (1976) 504.
10 B. L. Grung, *Proc. 15th Photovoltaic Specialists' Conf., Orlando, FL, May 1981*, IEEE, New York, 1981.
11 H. P. D. Lanyon, *Sol. Cells, 3* (1981) 289.

12 D. Redfield, *Sol. Cells, 3* (1981) 313.
13 J. G. Fossum, F. A. Lindholm and M. A. Shibib, *IEEE Trans. Electron Devices, 26* (1979) 1294.
14 M. Wolf, *Proc. IRE, 48* (1960) 1246.
15 S. M. Sze, *Physics of Semiconductor Devices*, Wiley, New York, 1979, p. 644.
16 J. P. McKelvey, *Solid State and Semiconductor Physics*, Harper and Row, New York, 1966, p. 463.
17 M. Wolf, *IEEE Trans. Electron Devices, 27* (1980) 751.
18 M. Wolf, *Proc. IEEE, 51* (1963) 674.
19 V. K. Jain and S. C. Jain, *Phys. Status Solidi A, 30* (1975) K69.
20 C. F. Gay, *Proc. 13th Photovoltaic Specialists' Conf., Washington, DC, June 5 - 8, 1978*, IEEE, New York, 1978, p. 444.
21 H. T. Weaver and R. D. Nasby, *Solid-State Electron., 22* (1979) 687.
22 J. Del Alamo, J. Eguren and A. Luque, *Solid-State Electron., 24* (1981) 415.
23 J. Michel, A. Mircea and E. Fabre, *J. Appl. Phys., 46* (1975) 5043.
24 J. Mandelkorn and J. H. Lamneck, Jr., *Proc. 11th Photovoltaic Specialists' Conf., Phoenix, AZ, May 6 - 8, 1975*, IEEE, New York, 1975, p. 36.
25 A. Sinha and S. K. Chattopadhyaya, *Solid-State Electron., 22* (1979) 849.
26 A. Agarwala, V. K. Tewary, S. K. Agarwal and S. C. Jain, *Solid-State Electron., 23* (1980) 1021.

Appendix A. Temperature degradation of V_{oc}

According to ref. A1 the emitter dark saturation current density is given by

$$J_{E0} = \frac{qn_{ie}^2 D_E}{N_D L_E}\left(\frac{S_F}{D_E/L_E} + \tanh W_E\right)\left\{1 + \left(\frac{S_F}{D_E/L_E}\right)\tanh W_E\right\}^{-1} \quad \text{(A1)}$$

The intrinsic carrier concentration n_{ie} is given in terms of the temperature and the band gap narrowing as [A2, A3]

$$n_{ie}^2 = CT^3 \exp\left\{-\left(\frac{E_g + \Delta E_g}{kT}\right)\right\} \quad \text{(A2)}$$

where C is a temperature-independent constant. Putting n_{ie}^2 from eqn. (A2) into eqn. (A1) and combining all the temperature-independent terms into a constant A, we obtain

$$J_{E0} = AT^3 \exp\left\{-\left(\frac{E_g + \Delta E_{gE}}{kT}\right)\right\} \quad \text{(A3)}$$

The value of A in eqn. (A3) is obtained by using $J_{E0} = 2 \times 10^{-12}$ A cm^{-2} [A4 - A6] at 300 K for any value of the emitter band gap narrowing ΔE_{gE}.

Similarly, putting n_{ie}^2 from eqn. (A2) into eqn. (1a) and assuming the band gap narrowing in the base for a doping level of about 10^{15} cm^{-3} to be zero, *i.e.* $\Delta E_g = 0$ in eqn. (A2), we obtain

$$J_{B0} = \frac{qBT^3 D_B}{L_B N_B}\left(\frac{S_{eff}'}{D_B/L_B} + \tanh W_B\right)\left\{1 + \left(\frac{S_{eff}'}{D_B/L_B}\right)\tanh W_B\right\}^{-1} \exp\left(-\frac{E_g}{kT}\right) \quad \text{(A4)}$$

where for silicon $B = 2.8 \times 10^{31}$ cm^{-6} K^{-3} [A2] and $E_g = 1.1$ eV.

S_{eff}' at a temperature T(K) for band gap narrowing ΔE_{gH} in a region is given by [A7]

$$S_{\text{eff}}' = S_{\text{eff}} \exp\left(\frac{\Delta E_{\text{gH}}}{kT}\right) \tag{A5}$$

Equations (A4) and (A5) were used in combination to calculate J_{B0}. After calculating J_{E0} and J_{B0} for a given value of ΔE_{gE} and ΔE_{gH} for a given temperature, we used eqn. (2) to calculate the value of V_{oc}. The value of J_{sc} for a back-surface field cell was taken to be equal to 45 mA cm^{-2} for 1 sun AM 0 illumination (Section 2).

References for Appendix A

A1 M. P. Godlewski, C. R. Baraona and H. W. Brandhorst, Jr., *Proc. 10th Photovoltaic Specialists' Conf., Palo Alto, CA, November 13 - 15, 1973*, IEEE, New York, 1974, p. 40.

A2 J. P. McKelvey, *Solid State and Semiconductor Physics*, Harper and Row, New York, 1966, p. 256.

A3 S. M. Sze, *Physics of Semiconductor Devices*, Wiley, New York, 1979, p. 27.

A4 H. P. D. Lanyon, *Sol. Cells, 3* (1981) 289.

A5 D. Redfield, *Sol. Cells, 3* (1981) 313.

A6 J. G. Fossum, F. A. Lindholm and M. A. Shibib, *IEEE Trans. Electron Devices, 26* (1979) 1294.

A7 C.-Y. Wu and W.-Z. Shen, *Solid-State Electron., 23* (1980) 209.